Article

Nature of the Chemical Bond between Metal Atoms and Oxide Surfaces: New Evidences from Spin Density Studies of K Atoms on Alkaline Earth Oxides

Mario Chiesa, Elio Giamello, Cristiana Di Valentin, Gianfranco Pacchioni, Zbigniew Sojka, and Sabine Van Doorslaer

J. Am. Chem. Soc., **2005**, 127 (48), 16935-16944• DOI: 10.1021/ja0542901 • Publication Date (Web): 11 November 2005

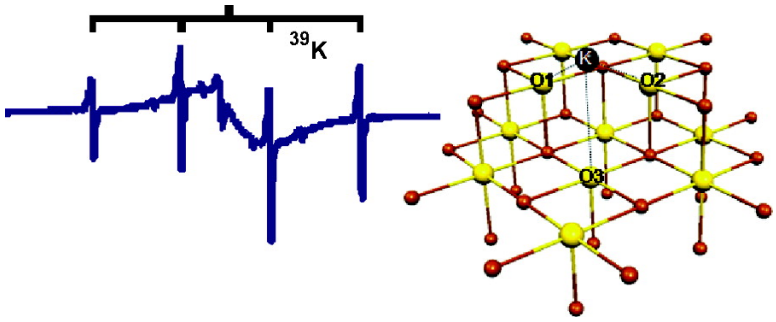

J|A|C|S
ARTICLES
Published on Web 11/11/2005

Nature of the Chemical Bond between Metal Atoms and Oxide Surfaces: New Evidences from Spin Density Studies of K Atoms on Alkaline Earth Oxides

Mario Chiesa,*,† Elio Giamello,† Cristiana Di Valentin,‡ Gianfranco Pacchioni,‡ Zbigniew Sojka,§ and Sabine Van Doorslaer||

Contribution from the Dipartimento di Chimica IFM, Università di Torino and NIS Centre of Excellence via P. Giuria 7, 10125, Torino, Italy, Dipartimento di Scienza dei Materiali, Università di Milano-Bicocca, via R. Cozzi 53, 20125 Milano, Italy, Department of Chemistry and Regional Laboratory of Physicochemical Analysis and Structural Research Jagiellonian University, ul. Ingardena 3, 30-060 Cracow, Poland, and Laboratory for Spectroscopy in Biophysics and Catalysis, Department of Physics, University of Antwerp, Universiteitsplein 1, B-2610 Wilrijk, Belgium

Received June 29, 2005; E-mail: m.chiesa@unito.it

Abstract: We have studied the interaction of K atoms with the surface of polycrystalline alkaline-earth metal oxides (MgO, CaO, SrO) by means of CW- and Pulsed-EPR, UV−Vis−NIR spectroscopies and DFT cluster model calculations. The K adsorption site is proposed to be an anionic reverse corner formed at the intersection of two steps, where K binds by more than 1 eV, resulting in thermally stable species up to about 400 K. The bonding has small covalent and large polarization contributions, and the K atom remains neutral, with one unpaired electron in the valence shell. The interaction results in strong modifications of the K electronic wave function which are directly reflected by the hyperfine coupling constant, $^{K}a_{iso}$. This is found to be a very efficient "probe" to measure the degree of metal-oxide interaction which directly depends on the substrate basicity. These results provide an original and general model of the early stages of the metal−support interaction in the case of ionic oxides.

1. Introduction

The chemical and physical properties of solids are related to the way in which the electron density is distributed over the valence shell of the constituent atoms.[1] Understanding the factors that influence this distribution is thus of primary importance in the development of functional materials with new, possibly controlled, electronic and chemical properties. A relevant example in this sense is constituted by the case of metal atoms supported on oxide substrates, a class of relevant materials which presents opportunities for a variety of challenging applications spanning from electronic micro devices to corrosion protection and catalysis.[2−6]

Metal atoms and clusters bound to oxide surfaces exhibit unique physical and chemical properties which directly stem from the interaction between the metal and the substrate. Catalytic activity and selectivity of metal particles certainly depend on the nature of the metal and on the size of the aggregate,[7] but the oxide support, far from being an inert host, does influence the electronic structure of deposited metal atoms through specific interactions with particular surface sites. This confers to the supported metal catalytic properties not observed for the free atom.

Metal−support interactions are expected to depend, for a given metal, on three main factors, i.e., the physical and chemical properties of the oxide (band structure and conductivity, acid−base character, nature of the cation), its morphological habit (type of exposed faces, presence of steps, kinks and other similar features), and finally, the defective state of the surface (presence of point defects such as ion vacancies and trapped electrons). Several authors have stressed in particular the relevance of surface point defects, namely anion vacancies or F centers, in the nucleation and growth of metal particles as well as in enhancing the catalytic activity of coinage metals deposited on oxide surfaces.[8−11] There is no doubt that anion vacancies play a paramount role in determining the reactivity

† Università di Torino and NIS Centre of Excellence.
‡ Università di Milano-Bicocca.
§ Department of Chemistry and Regional Laboratory of Physicochemical Analysis and Structural Research Jagiellonian University.
|| University of Antwerp.

(1) Hoffman, R. *Solids and Surfaces*; VCH Publishers Inc.: New York, 1988.
(2) Freund, H.-J. *Surf. Sci.* **2002**, *500*, 271.
(3) Campbell, C. T. *Surf. Sci. Rep.* **1997**, *27*, 3.
(4) Pacchioni, G.; Illas, F. In. Wieckowski, A., Savinova, E., Vayenas, C. G., Eds.; *Catalysis and Electrocatalysis at Nanoparticle Surfaces*; Dekker: New York, 2003.
(5) Henry, C. R. *Surf. Sci. Rep.* **1998**, *31*, 231.
(6) Judai, K.; Abbet, S.; Worz, A. S.; Heiz, U.; Henry, C. R. *J. Am. Chem. Soc.* **2004**, *126*, 2732.
(7) Che, M.; Bennet, C. O. *Adv. Catal.* **1989**, *36*, 55.
(8) Hakkinen, H; Abbet, W.; Sanchez, A.; Heiz, U.; Landman U. *Angew. Chem., Int. Ed.* **2003**, *42*, 1297.
(9) Heiz, U.; Bullock, E. L. *J. Mater. Chem.* **2004**, *14*, 564.
(10) Abbet, S.; Riedo, E.; Brune, H.; Heiz, U.; Ferrari, A. M.; Giordano, L.; Pacchioni, G. *J. Am. Chem. Soc.* **2001**, *123*, 6172.
(11) Yan, Z.; Chinta, S.; Mohamed, A. A.; Fackler, J. P.; Goodman, D. W. *J. Am. Chem. Soc.* **2005**, *127*, 1604.

of solid surfaces by triggering charge-transfer reactions either from or toward adsorbed species. Relevant examples are group VIII transition metal atoms (Rh, Pd) as well as IB elements (in particular Au) deposited on MgO surfaces. The former are active catalysts in the cyclotrimerization of acetylene to benzene,[12] whereas the latter promote the low-temperature oxidation of CO to CO_2.[13]

The role of surface F centers in modifying the properties of adsorbed metals has thus polarized the attention of researchers and only little attention, especially from the experimental side, has been devoted to investigate the role played by all possible sites present at the surface of a real oxide (which is generally a rather heterogeneous system) and, even more important, the nature of the chemical bond between the oxide surface sites and the metal.

MgO, a prototype of ionic insulating oxides for its simple structure, has been widely employed for fundamental investigations as it can be prepared in the form of thin film, single crystal, or as high surface area polycrystalline system. This oxide has morphological defective features such as steps, corners or reverse corners, which are known to be dominant irregularities at the surface of oxide polycrystals as well as thin oxide films.[14] Furthermore, it is the first member of the family of insulating alkaline-earth oxides, all having the same structure but different basicity. MgO and the other members of the series are thus ideal model systems to study the nature and structure of the surface sites and their impact on the metal-oxide chemical bond. As to the latter factor, the role of surface basicity assumes a particular importance. The substrate basicity, in fact, has been predicted, by ab initio theoretical calculations, to strongly affect the electronic properties of adsorbed metal atoms[15] and is in general known to have a direct influence on the electronic properties of surface stabilized species.[16] This effect has been experimentally studied in the case of Pt and Pd atoms supported on zeolites.[17] Although modifications of the metal *d*-band was related to the substrate basicity, a direct experimental measure of the influence of the basic character of the substrate on the electronic structure of deposited metal atoms is, to the best of our knowledge, still missing.

In this paper, we report a combined experimental and theoretical study on the interaction of a "probe" metal like K with the surface of polycrystalline MgO, CaO and SrO. By means of Continuous Wave (CW) and Pulsed Electron Paramagnetic Resonance (EPR) Spectroscopy on a ^{17}O enriched MgO sample, we show that isolated K atoms are relatively strongly bound to oxide anions at particular morphological irregularities of the surface. Extending the study to the other members of the family, we will show that the metal unpaired electron spin density, directly measured by EPR, can provide a quantitative measure of the degree of interaction between the metal and the surface. DFT calculations corroborate the experimental results and provide clear insights into the nature of the metal−support interaction.

The paper is organized as follows. In section 2 experimental and computational procedures are described. In sections 3.1 and 3.2, the results of CW- and pulsed EPR measurements on the interaction of K atoms with ^{17}O enriched MgO are reported. Section 3.3 is dedicated to the thermal stability and the optical spectra of the deposited atoms. 3.4 describes the interaction of K atoms with the surface of CaO and SrO. Section 3.5 reports experimental evidence about the nature of the trapping site, while a detailed analysis of $\boldsymbol{A}$ and $\boldsymbol{g}$ tensors is given in Section 3.6. Results of DFT calculations and a firm assignment of the adsorption site are presented in 3.7. In 3.8, the chemistry of the metal to surface interaction is rationalized within the general framework of solvation chemistry. Conclusions are drawn in the last section.

2. Experimental and Computational Details

2.1. Material Preparation and Experimental Methods. High surface area polycrystalline MgO, CaO and SrO oxides were prepared by slow decomposition of the corresponding hydroxides (MgO) and carbonates (CaO and SrO) in a vacuum and then activated at 1173 K in order to remove impurities as described elsewhere.[18] The isotopic enrichment of the MgO surface was carried out by successive hydration and dehydration cycles of the sample exposing the solid to vapors of $H_2{}^{17}O$ (86% isotopic enrichment supplied by Icon Services New Jersey).[19,20] Potassium metal shots were distilled in a vacuum to form a metal mirror in a separate part of the quartz cell used for EPR and UV−Vis−NIR measurements. The metal was evaporated on the sample "in situ" by heating the metallic mirror while keeping the powder at nearly room temperature.

CW-EPR spectra were recorded on a Bruker ESP 300E spectrometer equipped with a gas-flow cryostat (Oxford inc.) which allows the spectra to be recorded in the interval between 480 and 4 K. CW spectra were recorded at 1 mW microwave power, 100 kHz modulation frequency and 0.05 mT modulation amplitude. The CW-EPR spectra were simulated using the EPRsim32 program.[21]

All pulse-EPR spectra were recorded on a Bruker ESP380E spectrometer operating at a microwave (mw) frequency of 9.77 GHz and equipped with a liquid Helium cryostat (Oxford Inc.) The spectra were taken at 10 K. In all pulse EPR experiments, a repetition rate of 500 Hz was used. Hyperfine Sublevel Correlation (HYSCORE)[22] experiments were carried out with the pulse sequence $\pi/2 - \tau - \pi/2 - t_1 - \pi - t_2 - \pi/2 - \tau -$ echo with microwave pulse length $t_{\pi/2} = 16$ ns and $t_\pi = 16$ ns. The time intervals t_1 and t_2 were varied in steps of 8 ns starting from 96 ns. Three different τ values were used ($\tau = 184$, 248, and 328 ns). An eight-step phase cycle was used to eliminate unwanted echoes. The time traces of the HYSCORE spectra were baseline corrected with a third-order polynomial, apodized with a Hamming window and zero filled. After two-dimensional Fourier transformation, the absolute value spectra were calculated. The spectra were added for the different τ values in order to eliminate blind-spot effects. The HYSCORE spectra were simulated using a program developed at the ETH Zurich.[23]

UV−Vis−NIR (Varian Cary-5) spectra were recorded at room temperature on the same sample used for the EPR measurements.

2.2. Computational Details. Density Functional Theory (DFT) calculations have been carried out using the gradient corrected Becke's

(12) Judai, K.; Worz, A. S.; Abbet, S.; Antonietti, J. M.; Heiz, U.; Del Vitto, A.; Giordano, L.; Pacchioni, G. *Phys. Chem. Chem. Phys.* **2005**, *7*, 955.
(13) Yoon, B.; Hakkinen, H.; Landman, U.; Worz, A. S.; Antonietti, J. M.; Abbet, S.; Judai, K.; Heiz, U. *Science* **2005**, *307*, 403.
(14) Spoto, G.; Gribov, E. N.; Ricchiardi, G.; Damin, A.; Scarano, D.; Bordiga, S.; Lamberti, C.; Zecchina, A. *Prog. Surf. Sci.* **2004**, *76*, 71.
(15) Lopez, N. *J. Chem. Phys.* **2001**, *114*, 2355.
(16) Pacchioni, G.; Ricart, M. J.; Illas, F. *J. Am. Chem. Soc.* **1994**, *116*, 10152.
(17) Mojet, B. L.; Miller, J. T.; Ramaker, D. E.; Koningsberger, D. C. *J. Catal.* **1999**, *186*, 373.
(18) Purnell, I.; Chiesa, Farley, R. D.; M.; Murphy, D. M.; Rowlands, C. C.; Paganini, M. C.; Giamello, E. *Magn. Reson. Chem.* **2002**, *40*, 381.
(19) Chiesa, M.; Martino, P.; Giamello, E.; Di Valentin, C.; Del Vitto, A.; Pacchioni, G. *J. Phys. Chem. B* **2004**, *108*, 11529.
(20) Chiesa, M.; Giamello, E.; Di Valentin, C.; Pacchioni, G. *Chem. Phys. Lett.* **2005**, *403*, 124.
(21) Adamski, A.; Spalek, T.; Sojka, Z. *Res. Chem. Indermediat* **2003**, *29*, 793.
(22) Höfer, P.; Grupp, A.; Nebenfür, H.; Mehring, M. *Chem. Phys. Lett.* **1986**, *132*, 279.
(23) Madi, Z. L.; Van Doorslaer, S.; Schweiger, A. *J. Magn. Reson.* **2002**, *154*, 187.

three parameters hybrid exchange functional[24] in combination with the correlation functional of Lee, Yang, and Parr[25] (B3LYP). The MgO, CaO, and SrO surfaces were simulated by finite MO clusters (M = Mg, Ca, Sr) embedded in ±2 point charges (PC) which reproduce the Madelung potential at the adsorption site.[26] To avoid the artificial polarization of the O^{2-} anions at the cluster border,[27−30] the positive PCs at the interface were replaced by effective core potentials (ECPs)[31] which provide a representation of the finite size of the cation. The interface M^{2+} cations treated in this way are denoted in the following as M*. No basis functions are associated to these atoms.

For the MgO surface, various adsorption sites have been considered: regular (100) terraces, low coordinated ions (i.e., edge or step sites), other morphological defects such as corners and reverse corners (RC; these sites originate from the intersection of two steps). Notice that there are two types of reverse corners: one centered on a Mg cation and characterized by two O_{4c} and one O_{5c} anions forming a triangular adsorption site (anionic RC) and one centered on a O anion and characterized by two Mg_{4c} and one Mg_{5c} cations (cationic RC). For the heavier oxides CaO and SrO only terrace and anionic RC sites have been considered.

The clusters are embedded in an array of ∼3000 PC's fixed at the bulk lattice positions. The size of the quantum part is $Mg_9O_9Mg^*_{16}$ for a terrace, $Mg_{10}O_{10}Mg^*_{14}$ for an edge, $Mg_{12}O_{12}Mg^*_{17}$ for a step, $Mg_{12}O_{12}Mg^*_{18}$ for a double step, $Mg_4O_4Mg^*_6$ for a corner, and $Mg_{11}O_{11}Mg^*_{18}$ for an anionic reverse corner.

The Mg atoms near the adsorption site have been described with a 6-31G*[32] basis set while the remaining atoms have been treated with the 6-31G[32] basis. All the O atoms have been described with the 6-31+G*[32,33] basis. For the Ca and Sr cations, we used a small core ECP which treats explicitly the $3s^2$ $3p^6$ and $4s^2$ as valence electrons and the Lanl2dz basis set.[31] A d polarization function has been added on the Ca and Sr atoms first-neighbors of the adsorbing site (α_d = 0.57 for Ca and α_d = 0.42 for Sr). The basis set for K, 6-311+G*,[34] has been chosen in order to reproduce accurately the ionization potential (IP = 4.50 eV, exp. = 4.34 eV),[35] the polarizability ($\alpha = 41.5\ 10^{-24}$ cm^3, exp. = $43.4\ 10^{-24}$ cm^3)[35,36] and the isotropic hyperfine coupling constant (a_{iso} = 8.39 mT, exp. = 8.25 mT)[37] of the free K atom. The interaction energies have been corrected by the basis set superposition error (BSSE) using the counter-poise correction.[38] The hyperfine interaction, $\boldsymbol{A} = a_{iso} + \boldsymbol{T}$, of the electron spin with the nuclear spin (see below) have been determined and compared with the experimental values.

The calculations have been performed using Gaussian-03 program package.[39]

3. Results and Discussion

3.1. EPR Spectra of K/MgO. The exposure of carefully dehydrated MgO to K vapor caused the transparent oxide to turn deep blue. The first type of paramagnetic center observed at very low levels of K doping are F_s^+ centers (oxygen vacancies containing an unpaired electron) characterized by a narrow axial EPR signal at g value around 2.000 (the signal is evidenced in Figure 1). These centers have been characterized in detail in the past[40,41] and more recently by ab initio theoretical modeling[42] and we shall no longer discuss them here. By carefully dosing the amount of deposited metal the EPR spectrum reported in Figure 1a was observed. The spectrum is dominated by four lines arising from the hyperfine interaction of the K 4s valence electron with the ^{39}K nucleus (I = 3/2, 93.26%, g_K = 0.26099) and can readily be assigned to isolated K atoms. The presence of another quartet of lines of weaker intensity and smaller spacing is due to the ^{41}K isotope (I = 3/2, 6.73%, g_K = 0.14325). The apparent distortion of the hyperfine lines, most visible for the m_I = 3/2 transition, indicates some slight anisotropy of the magnetic parameters. The assignment was confirmed by computer simulation of the spectrum (Figure 1b), which was obtained by imposing two hyperfine quartets with coupling constants scaled according to the ratio of the nuclear magnetic moments of both isotopes (0.26099/0.14325 = 1.82) and intensities adjusted to their natural abundances.

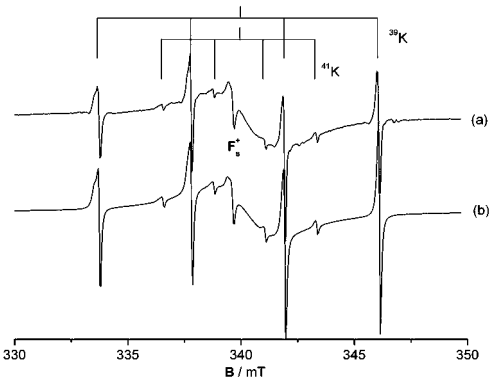

Figure 1. Experimental (a) and simulated (b) CW EPR spectra of K atoms deposited on MgO. The spectra are recorded at 77K.

The simulation was carried out assuming the following spin Hamiltonian

$$\mathscr{H} = \beta_e \boldsymbol{B}^T \cdot \boldsymbol{g} \cdot \boldsymbol{S} + \sum_i \boldsymbol{S}^T \cdot \boldsymbol{A}_i \cdot \boldsymbol{I}_i \qquad (1)$$

with virtually axial $\boldsymbol{g}$ and $\boldsymbol{A}$ tensors (g_z = 2.000, $g_{x,y}$ = 1.999 and $A_{x,y}$ = 3.988 mT, A_z = 4.092 mT). A narrow feature centered at g = 2.00, due to trapped electrons (in F_s^+ centers),[41]

(24) Becke, A. D. *J. Chem. Phys.* **1993**, *98*, 5648.
(25) Lee, C.; Yang, W.; Parr, R. G. *Phys. Rev. B* **1988**, *37*, 785.
(26) Pacchioni, G.; Ferrari, A. M.; Marquez, A. M.; Illas, F. *J. Comput. Chem.* **1997**, *18*, 617.
(27) Cundari, T. R.; Stevens, W. J. *J. Chem. Phys.* **1993**, *98*, 5555.
(28) Winter, N. W.; Pitzer, R. M. *J. Chem. Phys.* **1988**, *89*, 89.
(29) Nygren, M. A.; M. Petterson, L. G.; Barandiaran, Z.; Seijo, L. *J. Chem. Phys.* **1994**, *100*, 2010.
(30) Mejias, J. A.;. Marquez, A. M.; Fernandez Sanz, J.; Fernandez-Garcia, M.; Ricart, J. M.; Sousa, C.; Illas, F. *Surf. Sci.* **1995**, *327*, 59.
(31) Hay, P. J.; Wadt, W. R. *J. Chem. Phys.* **1985**, *82*, 270; Hay, P. J.; Wadt, W. R. *J. Chem. Phys.* **1985**, *82*, 299.
(32) Francl, M. M.; Petro, W. J.; Hehre, W. J.; Binkley, J. S.; Gordon, M. S.; De Frees, D. J.; Pople, J. A. *J. Chem. Phys.* **1982**, *77*, 3654.
(33) Clark, T.; Chandrasekhar, J.; Schleyer, P.v. R. *J. Comput. Chem.* **1983**, *4*, 294.
(34) Blaudeau, J.-P.; McGrath, M. P.; Curtiss, L. A.; Radom, L. *J. Chem. Phys.* **1997**, *107*, 5016.
(35) *CRC Handbook of Chemistry and Physics*; CRC Press: Boca Raton, FL, 1998.
(36) The atomic polarizability, α, has been computed from the induced dipole moment in the presence of a uniform electric field, according to the formula $\mu = \alpha \cdot F$.
(37) Koh, A. K.; Miller, D. J. *Atom. Data Nucl. Data Tables* **1985**, *33*, 235.
(38) Boys, S. F.; Bernardi, F. *Mol. Phys.* **1970**, *19*, 553.
(39) Frisch, M. J.; Trucks, G. W.; Schlegel, H. B.; Scuseria, G. E.; Robb, M. A.; Cheeseman, J. R.; Montgomery, J. A., Jr.; Vreven, T.; Kudin, K. N.; Burant, J. C.; Millam, J. M.; Iyengar, S. S.; Tomasi, J.; Barone, V.; Mennucci, B.; Cossi, M.; Scalmani, G.; Rega, N.; Petersson, G. A.; Nakatsuji, H.; Hada, M.; Ehara, M.; Toyota, K.; Fukuda, R.; Hasegawa, J.; Ishida, M.; Nakajima, T.; Honda, Y.; Kitao, O.; Nakai, H.; Klene, M.; Li, X.; Knox, J. E.; Hratchian, H. P.; Cross, J. B.; Bakken, V.; Adamo, C.; Jaramillo, J.; Gomperts, R.; Stratmann, R. E.; Yazyev, O.; Austin, A. J.; Cammi, R.; Pomelli, C.; Ochterski, J. W.; Ayala, P. Y.; Morokuma, K.; Voth, G. A.; Salvador, P.; Dannenberg, J. J.; Zakrzewski, V. G.; Dapprich, S.; Daniels, A. D.; Strain, M. C.; Farkas, O.; Malick, D. K.; Rabuck, A. D.; Raghavachari, K.; Foresman, J. B.; Ortiz, J. V.; Cui, Q.; Baboul, A. G.; Clifford, S.; Cioslowski, J.; Stefanov, B. B.; Liu, G.; Liashenko, A.; Piskorz, P.; Komaromi, I.; Martin, R. L.; Fox, D. J.; Keith, T.; Al-Laham, M. A.; Peng, C. Y.; Nanayakkara, A.; Challacombe, M.; Gill, P. M. W.; Johnson, B.; Chen, W.; Wong, M. W.; Gonzalez, C.; Pople, J. A. *Gaussian 03*, revision A.1; Gaussian, Inc.: Wallingford, CT, 2004.
(40) Giamello, E.; Ferrero, A.; Coluccia, S.; Zecchina, A. *J. Phys. Chem.* **1991**, *95*, 9385.
(41) Giamello, E.; Murphy, D. M.; Ravera, L.; Coluccia, S.; Zecchina, A. *J. Chem. Soc., Faraday Trans.* **1994**, *90*, 3167.
(42) Brazzelli, S.; Di Valentin, C.; Pacchioni, G.; Chiesa, M.; Giamello, E. *J. Phys. Chem. B* **2003**, *107*, 8498.

Table 1. Spin-Hamiltonian Parameters for K Atoms Deposited on Different Alkaline-Earth Oxides

	$g_{\|}$	$g_{\perp}$	$^{K}A_{\|}$/mT	$^{K}A_{\perp}$/mT	a_{iso}/mT	T_1/mT	T_2/mT	T_3/mT
MgO	2.000	1.999	4.18	4.12	4.14	−0.02	−0.02	+0.04
CaO	2.000	1.997	3.79	3.72	3.743	−0.023	−0.023	+0.046
SrO	1.992	1.989 1.986	2.66	2.69 2.73	2.69	−0.03	−0.0	+0.04

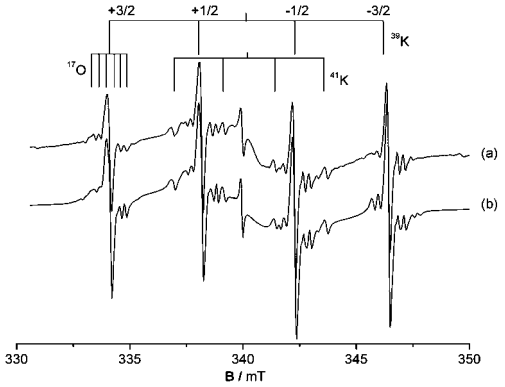

Figure 2. Experimental (a) and simulated (b) CW-EPR spectra of K atoms deposited on ^{17}O enriched MgO. Spectra recorded at 77 K.

together with a broad (ΔB = 35 G) absorption at g = 2.001 attributable to K metallic clusters[43] were also introduced in the simulation for the sake of completeness. The nature of these signals has already been discussed in the literature[41,43] and is outside the scopes of the present paper. The set of spin Hamiltonian parameters used in the simulation is listed in Table 1.

To explore the nearest environment of surface bound K atoms and ascertain the nature of the surface binding sites, experiments on a ^{17}O isotopically enriched MgO sample were carried out. In principle, the overlap between the K atom and the matrix orbitals will give rise to superhyperfine interaction between the unpaired electron and surface $^{25}Mg^{2+}$ ions (the only nucleus bearing nuclear magnetic moment, I = 5/2, 10% natural abundance). However, no trace of such an interaction could be observed in the EPR spectrum reported in Figure 1. On the contrary, the signature of the superhyperfine interaction between K atoms and ^{17}O nuclei is clearly visible in the EPR spectrum recorded after adsorption of K vapors on the ^{17}O enriched MgO (Figure 2a). Due to the coupling with the ^{17}O nucleus (I = 5/2) the ^{39}K hyperfine lines are further split into a sextet equally spaced by about 0.28 mT. This result provides firm experimental evidence that isolated K atoms are bound to surface oxygen anions. Previous studies[19,20] have shown that the isotopic exchange is restricted to the most active sites of the surface or their immediate surroundings but the extent of enrichment in the ^{17}O isotope at the surface is actually unknown (vide infra). To investigate further the local structure of isolated K atoms Electron Spin−Echo Envelope Modulation (ESEEM) experiments have been carried out.

3.2. ESEEM Studies of K/Mg^{17}O. Figure 3a shows the HYSCORE spectrum of K atoms deposited on ^{17}O enriched MgO taken at observer position 350.7 mT which coincides with the m_I = −1/2 transition of the spectrum in Figure 2 (similar results were obtained for other magnetic-field settings). The spectrum contains three sets of cross-peaks resulting from

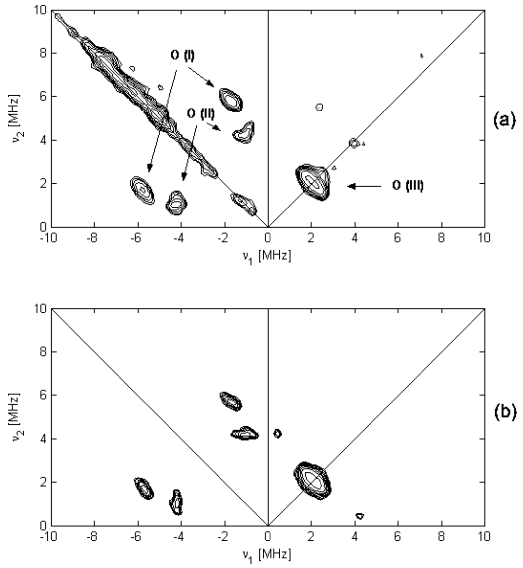

Figure 3. Experimental (a) and simulated (b) HYSCORE spectra of K atoms deposited on ^{17}O enriched MgO. Spectra recorded at 10K.

Table 2. ^{17}O Hyperfine Tensor Derived from the Simulation of the HYSCORE Spectrum

	^{17}O A tensor/mT			
	a_{iso}	T_1	T_2	T_3
O(I)	−0.28	+0.03	+0.03	−0.06
O(II)	−0.15	+0.02	+0.02	−0.04
O(III)	−0.01	+0.014	+0.014	−0.028

interactions with distinct ^{17}O nuclei. Two sets of off-diagonal cross-peaks are found in the (−,+) quadrant at approximately (−5.8,1.7) and (−1.7,5.8) MHz, and at (−4.2,1.1) and (−1.1,4.2) MHz, respectively. As expected in the case of a strong hyperfine coupling the cross-peaks are separated by approximately 2 ν_O. The assignment of the above-mentioned signals to ^{17}O nuclei are further corroborated by hyperfine-decoupling experiments (see Supporting Information). A third signal (O(III)), is found in the (+,+) quadrant and is centered at (ν_O,ν_O), where ν_O is the ^{17}O nuclear Zeeman frequency, displaying a maximum width of about 1.2 MHz. To establish the nature of this signal, in particular if it can be assigned to the interaction with a specific ^{17}O nucleus or rather is due to the contribution of remote ^{17}O nuclei, we performed a detailed simulation analysis considering different situations. The analysis (reported in the Supporting Information) shows that several possibilities for the simulation of the O(III) signal can be considered (and we show one) but that the width of the ridge can only be reproduced if, together with the contribution of remote nuclei, the presence of a near ^{17}O is taken into account. The interaction with each of the ^{17}O nuclei was simulated separately and the individual traces added together (Figure 3b, Table 2). The details of the simulation are reported in the Supporting Information. The nuclear quadrupole couplings were found to be small (e^2qQ/h ≅ 1 MHz), consistent with the narrow form of the single quantum cross-peaks and

(43) Edmonds, R. N.; Edwards, P. P.; Guy, S. C.; Johnson, D. C. *J. Phys. Chem.* **1984**, *88*, 3764.

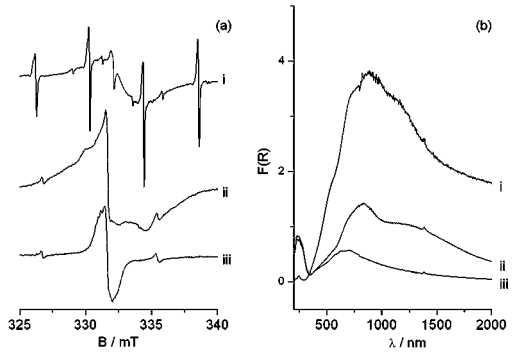

Figure 4. CW-EPR (a) and UV−Vis−NIR spectra (b) of K atoms recorded after different annealing treatments; (i) sample as prepared, (ii) annealed at 473K for 30 min, (iii) annealed at 473K for 60 min.

the lack of multiple quantum features in the HYSCORE spectra. The values fall within the typical range reported for inorganic materials.[44] The hyperfine values were used to simulate the CW-EPR spectrum reported in Figure 2. The best fitting was obtained assuming an isotopic enrichment of about 10%.

The extra resolution provided by the HYSCORE spectra clearly proves that *single K atoms are bound at surface sites where they interact with at least three oxygen ions.*

3.3. Thermal Stability and Optical Spectra of K/MgO. The temperature stability of the ^{39}K monomeric species was evaluated by recording EPR spectra in the temperature range between 4 and 380 K (see Supporting Information). The ^{17}O superhyperfine structure is not smeared out even at elevated temperatures indicating that the contact between the K atom and the surface oxygen ions constituting the hosting site is still preserved up to 380 K. *It is important to stress the high thermal stability of the trapped K atoms.* Using a Redhead equation with a preexponential factor 10^{13}, this corresponds to a K−MgO binding energy of about 1 eV.

Aiming to understand the electronic structure of trapped K in more detail we coupled CW-EPR with UV−Vis−NIR in situ measurements. The corresponding spectra recorded at RT are shown in Figure 4a and 4b. The CW-EPR spectrum of isolated K atoms on MgO, previously described (Figure 4a-i), is accompanied by a broad optical absorption with maximum at λ = 870 nm (Figure 4b-i). Annealing of the sample at 473 K for 30 min causes the disappearing of the ^{39}K hyperfine quartet and the broadening of the EPR signal (Figure 4a-ii, 4a-iii). This effect can be explained assuming that a considerable degree of mobility is induced on the surface as the temperature is increased, so that K atoms tend to aggregate to form clusters. The collapse of the ^{39}K hyperfine structure is paralleled by the progressive disappearance of the optical absorption band centered at 870 nm (Figure 4bii, 4biii). This strongly suggests that the K hyperfine quartet, which is diagnostic of isolated single metal species, is correlated with the band at 870 nm and that both the EPR and the optical spectra arise from the same species. The observed optical absorption with maximum at 870 nm can then be understood in term of a K 4*s* → 4*p* transition where the two electronic levels are strongly modified with respect to the gas phase (the gas phase 4*s* → 4*p* transition falls at 775 nm). These results indicate that decreasing of the spin density at the nucleus is accompanied by a red shift in the optical absorption band. A similar situation has been found in the case of alkali metals trapped in a wide variety of matrixes. [45]

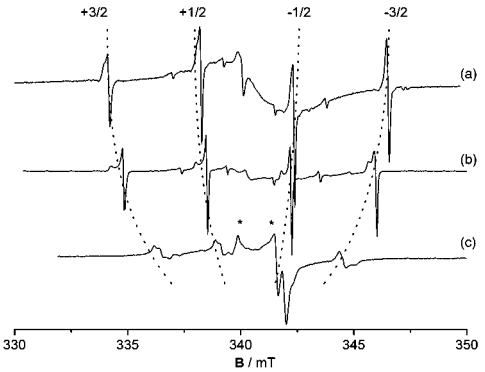

Figure 5. CW-EPR spectra of K atoms deposited on MgO (a), CaO (b), SrO (c). The spectra were recorded at 77 K. To evidence the variation of the hyperfine coupling constants across the series, the spectra have been centered at the same *g* value (g = 2.000).

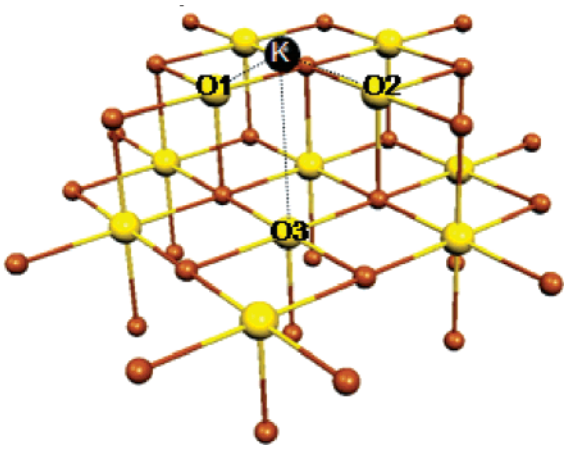

Figure 6. Cluster model for one K atom adsorbed on the anionic reverse corner. Black sphere for the K atom, small brown spheres for Mg atoms and yellow spheres for O atoms.

3.4. Interaction of K with CaO and SrO Surfaces. K deposition experiments were carried out also on the more basic CaO and SrO oxides. The EPR spectra recorded at 77 K are shown in Figure 5. The spectra were simulated under the same assumptions as in the case of MgO and the extracted parameters are collected in Table 1. In all cases, the dominant signal corresponds to monoatomic isolated K species. An impurity signal is present in the spectrum of K deposited on SrO (indicated with an asterisk in Figure 6c).

The ^{39}K hyperfine structure is significantly altered passing from MgO to SrO. The $^{K}a_{iso}$ value dropped from 4.14 mT for MgO to 3.74 mT for CaO and to 2.69 mT for SrO. Passing from MgO to SrO the decrease in the ^{39}K hyperfine coupling was accompanied by a decrease in the *g* value and an increase in the anisotropy of both ***g*** and ***A*** tensors. Eventually, in the case of the most basic SrO, a clearly orthorhombic spectrum was observed, consistent formally with a C_{2v} local symmetry of the hosting site.

3.5. Surface Trapping Sites. The first important information which comes from EPR and ESEEM spectra of K atoms on ^{17}O enriched MgO, Table 2, concerns the nature of the surface trapping site. HYSCORE spectra provide in fact direct experi-

(44) Lemaitre, V.; Smith, M. E.; Watts, A. *Solid State Nucl. Mag.* **2004**, *26*, 215.

(45) Catterall, R.; Edwards, P. P. *J. Phys. Chem.* **1980**, *84*, 1196.

mental evidence that K atoms are bound at surface oxygen anions. In the effort of establishing the nature of the trapping site two possibilities should be considered: (a) all the HYSCORE signals come from $^{17}O^{2-}$ within a single site; (b) different sites are responsible for the different ^{17}O spectral features. The second possibility requires that the g and K hyperfine values of the different species fall within the EPR line width ($\leq$0.12 mT) implying that the spin-Hamiltonian parameters are quasi the same. This suggests that if different sites are present they cannot have fundamental differences. We will try to address this issue with the help of DFT calculations. Estimate of the geometrical parameters relating the K−O distance can be obtained from the ^{17}O dipolar tensors. Considering a pure point-dipolar through space interaction the dipolar tensor ([$2T - T - T$]) is given by the following:

$$T = (\mu_0/4\pi)g_e g_n \beta_e \beta_n / r^3 \mathrm{h} \tag{2}$$

where r is the distance between the unpaired electron and the ^{17}O nucleus. A distance of about 2.2−2.5 Å can be estimated from eq 2 between the K atom and O(I) and O(II) respectively while an underlimit of 2.6 Å can be set for O(III) (see Supporting Information).

Some words of caution concerning the hosting sites for the other two oxides (CaO and SrO) are required. While for MgO a complete set of experimental data was obtained, the same was not possible for the other two oxides. Thus, we can only assume at this stage that the same adsorption site stabilizes K atoms on MgO, CaO, and SrO surfaces.

3.6. Analysis of *g* and *A* Tensors. *g* Tensor. The g values of K atoms on MgO were close to the gas-phase value g_J = 2.0023, as it may be expected for a species possessing no orbital angular momentum with the nominally perturbed $^2S_{1/2}$ ground state. The slight negative shift $\Delta g_{x,y} = -0.0023(4)$ is indicative of the spin−orbit induced coupling with empty states. The slight anisotropy of the ^{39}K hyperfine tensor with the largest departure along the z direction can be accounted for by a SOMO orbital with a_1 symmetry, bearing mainly K $|4s\rangle$ character with small admixture of $c|4p_z\rangle$ orbital. In second-order perturbation theory the shift of the components of the ***g*** tensor from the free electron value is given by

$$\Delta g_{ij} = 2\lambda_K \sum_n \langle n|L_i|\mathrm{SOMO}\rangle\langle \mathrm{SOMO}|L_j|n\rangle/(E_{\mathrm{SOMO}} - E_n) \tag{3}$$

where $\lambda_K = 39\ \mathrm{cm}^{-1}$ is the K spin−orbit coupling constant and L_i are components of the angular momentum operator. Because of the symmetry restrictions, the matrix elements of L_z between the a_1 ground state and other states vanish. On the other hand, the $L_{x,y}$ operator connects the ground state with $|p_{y,x}\rangle$ states, giving rise to the small shift of g value in these directions: $g_z \cong g_e$ and $g_{y,x} \cong g_e - (2c^2\lambda_K/\Delta E_{s-p})$. Thus, $g_z > g_{y,x}$ consistent with the experimental g tensor and its anisotropy (which is observed to grow going from MgO to SrO) is expected to increase with decreasing the 4s−4p energy gap.

^{39}K hyperfine tensors. The hyperfine tensor of the monomeric K center is fully consistent with the ground-state deduced for the analysis of the ***g*** tensor. The experimental $^K\boldsymbol{A}$ can be decomposed in the usual way into the isotropic Fermi contact term $^Ka_{iso}$ and the anisotropic traceless dipolar term $^K\boldsymbol{T}$ = ($-T$, $-T$, $2T$)

$$^K\boldsymbol{A} = {}^Ka_{iso}\mathbf{1} + {}^K\boldsymbol{T} \tag{4}$$

with

$$^Ka_{iso} = \frac{8\pi}{3} g_e \beta_e g_K \beta_n |\Psi_{(0)}|^2 \tag{5}$$

and

$$^K\boldsymbol{T} = g_e \beta_e g_K \beta_n \frac{1}{\langle r^3\rangle_{4p}} \times \left[-\frac{2}{5}, -\frac{2}{5}, \frac{4}{5}\right] \tag{6}$$

The isotropic pseudocontact interaction $P\langle g\rangle$ and dipolar through space term could be neglected here as being insignificant. Further analysis of hyperfine structure is possible only if the signs of the $^K\boldsymbol{A}$ tensor components are known. The only acceptable combination is obtained assuming the same sign for all the elements. Other combinations lead to unreasonably low $^Ka_{iso}$ values, in contradiction with the predominantly 4s character of the SOMO. Since the nuclear magnetic moment of ^{39}K is positive ($g_K > 0$), the sign of the hyperfine constants was taken to be positive (this choice is in agreement with DFT calculations, section 3.7), thus the decomposed $^K\boldsymbol{A}$ tensor assumes the form

$$^KA/g\beta_e = \begin{vmatrix} +4.12 & & \\ & +4.12 & \\ & & +4.18 \end{vmatrix}$$
$$mT = 4.14 + \begin{vmatrix} -0.02 & & \\ & -0.02 & \\ & & +0.04 \end{vmatrix} mT \tag{7}$$

The $^K\boldsymbol{A}$ tensor for K on CaO and SrO can be analyzed in an analogous way and the results are reported in Table 1.

As discussed above, the small dipolar component can be associated with ($|4s\rangle + c|4p_z\rangle$) hybridization allowed in C_{2v} symmetry. As the 4s and 4p orbitals become closer due to interaction with the oxygen ligands, the mixing coefficient c is enhanced, giving rise to a slightly increased anisotropy of the hyperfine coupling for CaO and SrO in comparison to MgO, in analogy to the ***g*** tensor. However, it should be stressed that the small T values indicate that, even though a small dipolar character is acquired by the adsorbed atom, the SOMO is predominantly 4s in character.

The extracted $^Ka_{iso}$ and ^KT components may be compared with the corresponding atomic values for assessment of the spin density repartition on the K 4s and 4p orbitals. In the case of MgO, substituting of numerical values yields $^K\rho_{4s} = {}^Ka_{iso}/{}^KA°_{iso} = 4.18\ \mathrm{mT}/8.24\ \mathrm{mT} = 0.502$ and $^K\rho_{4p} = {}^KT/{}^KT° = 0.035\ \mathrm{mT}/1.86\ \mathrm{mT} = 0.01$; one can deduce that in total the unpaired electron spin density $^K\rho_{total}$ (MgO) = $^K\rho_{4s} + {}^K\rho_{4p} = 0.503$ is reduced by more than 50% with respect to the unperturbed, gas-phase atom. The reduction of the spin density is even higher for the CaO and SrO: $^K\rho_{total}$(CaO) = 0.454 and $^K\rho_{total}$(SrO) = 0.326.

The reduction of the electron spin density at the K nucleus, relative to the atomic value, may indeed be understood in term of delocalization, although this implies that the remaining part of the spin density should give rise to a hyperfine interaction with matrix nuclei bearing a nuclear magnetic moment. For the ^{17}O-enriched MgO sample a superhyperfine interaction with at

Table 3. Computed Adsorption Energy and Hyperfine Coupling Constants, A, for a K Atom Adsorbed on Various Sites of the MgO Surface

		^{39}K ***A*** tensor/mT					^{17}O ***A*** tensor/mT				
MgO site	D_e[a]/eV	Spin	a_{iso}	T_1	T_2	T_3	site	a_{iso}	T_1	T_2	T_3
terrace	0.20	1.14	6.50	−0.02	−0.02	0.04	O_{5c}	−0.73	0.08	0.08	−0.16
edge	0.37	0.84	5.96	−0.03	−0.01	0.04	O_{4c}	−1.83	0.16	0.10	−0.26
step	0.45	1.03	5.53	−0.03	−0.01	0.04	O_{4c}	−1.64	0.18	0.10	−0.28
							O_{5c}	−0.57	0.07	0.07	−0.14
Double step	0.73	0.96	4.49	−0.04	0.01	0.03	O_{4c}	−1.69	0.21	0.09	−0.30
Corner	0.93	0.97	4.14	−0.02	−0.02	0.04	O_{3c}	−1.88	0.08	0.08	−0.16
Rev. corner	1.11	1.13	3.16	−0.05	−0.05	0.10	O_{4c}	−0.82	0.09	0.07	−0.16
							O_{5c}	−0.26	0.04	0.04	−0.08

[a] Corrected by the BSSE.

Table 4. Computed Hyperfine Coupling Constants, A, for a K Atom Adsorbed on the Anionic Reverse Corner of the MgO, CaO, and SrO Surfaces

	^{39}K ***A*** tensor/mT				$^{17}O_{4c}$ ***A*** tensor/mT				$^{17}O_{5c}$ ***A*** tensor/mT			
	a_{iso}	T_1	T_2	T_3	a_{iso}	T_1	T_2	T_3	a_{iso}	T_1	T_2	T_3
MgO	3.16	−0.05	−0.05	0.10	−0.82	0.09	0.07	−0.16	−0.26	0.04	0.04	−0.08
CaO	2.35	−0.06	−0.06	0.12	−0.38	0.07	0.06	−0.13	−0.16	0.04	0.04	−0.08
SrO	2.01	−0.06	−0.06	0.12	−0.28	0.05	0.05	−0.10	−0.15	0.03	0.03	−0.06

least three surface oxygen anions was detected. However, the observed hyperfine coupling constants cannot be reconciled with the spin density expected onto the matrix ions, if the classic delocalization model was valid. The experimental values are in fact at least one and a half order of magnitude lower than those predicted according to standard procedures of spin density repartition. This fact thus excludes that the origin of the lowered spin density observed at the K nucleus is due to a proper spin delocalization mechanism.

3.7. DFT Calculations and Assignment of Adsorption Site. The results described in the previous section can be summarized as follows: (a) K atoms are bound to at least three surface oxygen anions (section 3.2). They are thermally stable up to ~400 K corresponding to a binding energy of about 1 eV; (b) surface bound K species are subject to large perturbations arising from the strong interaction with the substrate; (c) the modification of the electron wave function is related to the basic character of the oxide. What remains to be answered is the structure of the adsorption site, the origin of the large thermal stability, and the nature of the K−MgO bonding, with particular attention to the possible occurrence of charge transfer to or from the surface. To answer these questions, we have performed DFT calculations on atomistic models.

The adsorption properties of a K atom bound to a five-coordinated oxide anion of MgO, CaO, SrO (terrace site) have been computed (see Supporting Information). For all the three oxides the bonding is found to be extremely weak, (0.20 eV on MgO, 0.28 eV on CaO, and 0.29 eV on SrO), and incompatible with the thermal stability observed experimentally. The second aspect which is in clear contradiction with the experiment is the a_{iso} value which is 6.5 mT (MgO), 6.1 mT (CaO), and 5.9 mT (SrO) while experimental values fall in the range between 2.7 mT (SrO) and 4.1 mT (MgO).

These data are sufficient to exclude that K atoms can be stabilized at regular terrace sites, and strongly suggest that defective sites may be involved.

The analysis of the possible defect sites involved has been done by placing K on various defective features of the MgO surface, Table 3. We assume that the conclusions obtained on this oxide are valid also for the heavier alkaline-earth oxides. The sites considered are, beside the terrace, steps, edges, corners, reverse corners. Not surprisingly, a lower coordination of the oxide anion to which K is bound results in a stronger bonding: on an edge (D_e = 0.37 eV) or on a step (D_e = 0.45 eV), the binding is almost twice that on a terrace; on a corner (D_e = 0.93 eV) the bond strength is more than four times larger than on a terrace. We also considered unusual sites such as a double step where K can interact simultaneously with two O_{4c} anions. The binding at this site, 0.71 eV, is about twice that on a normal step. Among these values of binding energies, only that found for a corner site is high enough to ensure stability at RT. However, the hypothesis that K is stabilized at corner sites is not fully consistent with the HYSCORE spectra (vide infra). The highest energetic stability is found for K interacting with an anionic RC, D_e = 1.11 eV, Figure 6 and Table 3. In this site K interacts with two O_{4c} ions (by about 0.45 eV each, according to step site binding energy, Table 4) and, less strongly with the basal O_{5c} center (0.2 eV, according to terrace site binding energy, Table 4). These three interactions seem to be nearly additive since they sum up to the total binding energy of 1.1 eV. Reverse corners are present in relatively high numbers on high surface area MgO.[46] The high stability computed at these sites, fully compatible with the persistence of the adsorbed species at RT, makes the anionic RC the best candidate to explain the presence of isolated K atoms on the MgO surface.

The other parameters to consider for the assignment of the adsorption site are the hfcc's for ^{39}K and ^{17}O. There is a clear correlation between bond strength and the $^{K}a_{iso}$ value: the highest is D_e, the smallest is $^{K}a_{iso}$, Table 4. However, it has to be stressed that the large changes in D_e do not reflect a change in the K spin population. Mulliken population analysis shows that nearly one unpaired electron occupies the K orbitals. Therefore, the reduction in $^{K}a_{iso}$ is due to other mechanisms, in particular to the strong intra-atomic polarization and expansion of the electron cloud. For the two most stable MgO sites considered, corner and reverse corner, $^{K}a_{iso}$ is 4.14 mT and 3.16 mT, respectively, Table 4. The former value is equal to the

(46) Ricci, D.; Di Valentin, C.; Pacchioni, G.; Sushko, P. V.; Shluger, A. L.; Giamello, E. *J. Am. Chem. Soc.* **2003**, *125*, 738.

Table 5. Computed Adsorption Properties for K Adsorbed on the Anionic Reverse Corner of MgO, CaO, and SrO Surfaces

	D_e[a] eV	spin[b] K	IP_v[c] eV	IP_a[d] eV	r(K–O1)[e] Å	r(K–O3)[e] Å
MgO	1.11	1.13	2.36	2.25	2.61	4.04
CaO	1.40	0.94	1.88	1.75	2.57	3.76
SrO	1.37	1.07	1.68	1.53	2.59	3.32

[a] Corrected by the BSSE. [b] Obtained from Mulliken analysis. [c] Vertical ionization potential. [d] Adiabatic ionization potential. [e] see Figure 6.

experimental one, however the $^{17O}a_{iso}$ (−1.88 mT) is very far from the experimental value of 0.28 mT.

A better agreement is found for the anion RC site. In this case, we need to assume that the HYSCORE ^{17}O signals (Figure 3) are due to O^{2-} ions within the same site, which is not inconsonant with the experimental spectrum. In Table 5 we give the K−O distances for a K atom adsorbed on a RC on the MgO, CaO, and SrO surfaces. It turns out that the K−O_{4c} distance is nearly constant along the series (around 2.6 Å), while the distance from the basal O_{5c} ion changes considerably from 4.04 Å in MgO, to 3.32 Å in SrO, Table 5. This is because the augmented lattice parameter in the heavier oxides favors the accommodation of the K atom into the cavity formed at the intersection of two steps, Figure 6. The computed values for the RC site of MgO are compatible with those deduced from the HYSCORE experiment, considering the approximations inherent to the procedure adopted: 2.2−2.5 Å for r(K−O_{4c}) (2.61 Å in the calculations), while the distance of 4.04 Å obtained from the calculations provides an acceptable solution for the simulation of the O(III) signal (see Supporting Information). On the basis of this analysis we propose that the anion RC is a very likely candidate for the adsorption site: it is relatively abundant, strongly binding, and gives hyperfine coupling constants with ^{39}K and K−O distances in acceptable agreement with the experiment. We wish to emphasize, however, that all the conclusions on the nature of the K−MgO interaction and the description of the electronic structure of surface bound alkali atom states (vide infra) remain valid regardless to the precise nature of the trapping site.

The cationic counterpart of the reverse corner site was first proposed by some of us in order to explain electron trapping phenomena observed upon irradiation of the solid in the presence of molecular hydrogen[46] and upon adsorption of Na atoms.[42] In this latter case, the cationic reverse corner was suggested to play an important role by inducing partial electron transfer from the metal to the surface, with consequent reduction of the metal hyperfine coupling constant. However, in total agreement with what has been computed for K in the present study, the anionic reverse corner was found to most strongly bind the Na atom and, even in the absence of any charge transfer, to considerably lower its hyperfine coupling constant, in agreement with experimental results.[41] Thus, it is likely that the importance of the interaction of Na with the anionic reverse corner has been underestimated in our previous study.

An important consequence of the bonding of K to a RC site of MgO, CaO, and SrO, is the strong reduction of the vertical IP which goes from 4.5 eV in gas-phase to 2.36 eV on MgO, 1.88 eV in CaO and 1.68 eV in SrO. Similar values are found for the adiabatic IP, showing a modest surface relaxation after the ionization, Table 5. The change in IP is connected to the destabilization of the ns level of the alkali atom due to the Pauli repulsion with the surface. This very phenomenon is also at the origin of the reduced $^{K}a_{iso}$ as well as of the red-shift in the optical bands observed experimentally and will be discussed in detail in section 3.8. Recent ab initio calculations on the optical transitions of Cu atoms adsorbed on MgO have found the same effect.[47]

The calculated hyperfine coupling constant for the O_{4c} nucleus is small, and decreases along the series of the investigated oxides, Table 4. An even smaller coupling is found with the basal O_{5c} ion, Table 4. Also in this case, however, we notice a quantitative discrepancy since the calculated $a_{iso} = -0.82$ mT for the O_{4c} ion of MgO is, nearly three times larger than the experimental value (0.28 mT). This discrepancy seems to indicate an overestimation of the K−O covalent character, i.e., an excessive delocalization of the unpaired electron, a well-known phenomenon in DFT calculations.[48] This is further proven by the fact that we calculated a small but nonzero value of $a_{iso}(^{25}Mg) \approx 0.4$ mT with the nearest neighbor Mg ions which is not observed experimentally.

Finally, we consider the evolution of the hyperfine coupling constants for K adsorbed on RC sites along the series MgO, CaO, SrO. The computed $a_{iso}(^{39}K)$ is 3.16 mT for MgO, 2.35 mT for CaO, and 2.01 mT for SrO, Table 4. These have to be compared with the experimental values, 4.14 mT, 3.74 mT, and 2.69 mT for MgO, CaO, and SrO, respectively, Table 1. Even though the computed values are systematically underestimated with respect to the experiment, for the reasons described above, the experimental trend is well reproduced. The calculations also correctly predict a very small value for the dipolar part of the hfcc with ^{39}K, Table 4, in full agreement with the experiment.

3.8. Nature of K Atoms Bound at the MgO Surface−Expanded Atom Model. To understand our results, it is appropriate to set comparison to other systems such as matrix isolated or solvated alkali metal atoms.[49,50] The solvent, being a liquid or a solid, exerts effects on the electronic properties of matrix bound states which range from small perturbations of the electron wave function brought about by dispersion or repulsive forces, as observed for alkali metals trapped in rare gases,[49,50] to dramatic changes arising from strong atom-solvent interactions as in the case of alkali metals trapped in different polar solvents.[51] These solvated atoms retain the recognizable properties of the gas-phase atom but are subject to considerable perturbations by the host medium and are of particular relevance to our case.

Just as we observe in our system, solvated alkali atoms are characterized by a decrease in the spin density at the metal nucleus which is accompanied by a red shift in the optical absorption band.[52] It is interesting to note that the same effect is observed in the case of gas-phase S excited states of the alkali metals.[53] Using data on hyperfine coupling constants for various nS states of K in the gas phase reported by Kopfermann[54] a

(47) Del Vitto, A.; Sousa, C.; Illas, F.; Pacchioni, G. *J. Chem. Phys.* **2004**, *121*, 7457.
(48) Pacchioni, G.; Frigoli, F.; Ricci, D.; Weil, J. A. *Phys. Rev. B* **2001**, *63*, 054102.
(49) Goldsborough, J. P.; Koehler, T. R. *Phys. Rev.* **1964**, *133A*, 135.
(50) Schrimpf, A.; Sulzer, G.; Stockmann, H−J.; Ackermann, H. *Phys. Lett.* **1985**, *110A*, 327.
(51) Catterall, R.; Edwards, P. P. *Chem. Phys. Lett.* **1976**, *42*, 540; **1976**, *43*, 122.
(52) Catterall, R.; Slater, J.; Seddon, W. A.; Fletcher, J. W. *Can. J. Chem.* **1976**, *54*, 3110.
(53) Gupta, R.; Happer, W.; Lam, L. K.; Svanberg, S. A. *Phys. Rev.* A **1973**, *8*, 2792.
(54) Kopfermann, H. *Nuclear Moments*; Academic Press: New York, 1968.

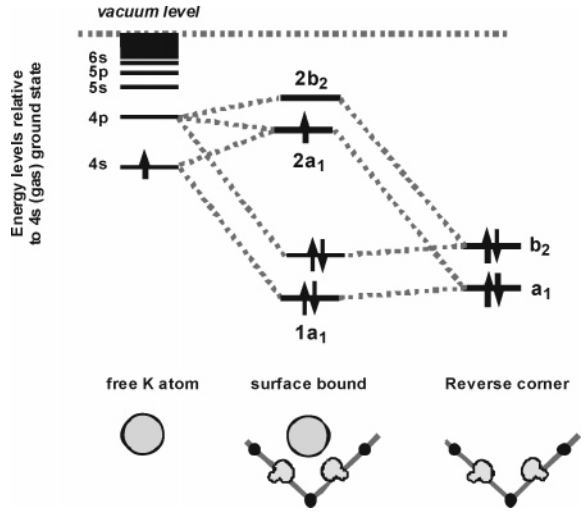

Figure 7. MO scheme for K atoms bound at anionic reverse corner sites. The 4s (2a1) and 4p (2b2) levels of the bound species have been set with respect to the corresponding gas-phase values making use of the Kopferman equation and of the electronic spectra.

simple empirical formula can be obtained, which relates the binding energy of the valence electron (relative to the gas phase 4s level) to the hyperfine coupling. Assuming the experimental red-shift of 870 nm (1.42 eV) as entirely due to the destabilization of the 4s orbital, $^{K}a_{iso} = 4.12$ mT was obtained, which compares very well with the experimental $^{K}a_{iso} = 4.14$ mT. Thus we may conclude that indeed, the real mechanism responsible for both the reduction of the spin density at the ^{39}K nucleus and the red shift in the optical absorption band is principally due to the pronounced shift in energy of the 4s level, caused by the interaction with the surface and not by direct delocalization of the spin density onto the matrix. The situation can be qualitatively described in terms of a simple molecular orbital scheme,[55] Figure 7, where the net result of the bonding interaction is to destabilize the K 4s level as well as allowing some degree of electron spin delocalization on the oxide anions. This implies that the K 4s level is lifted in energy becoming spatially more diffuse. In this "expanded atom" state the unpaired electron spin density at the nucleus is reduced with respect to the free atom and a reduced hyperfine coupling constant is observed without invoking any metal to surface electron transfer. These results also explain the EPR spectra of other members of group I metals adsorbed on MgO observed by some of us in the past.[56−58] The interaction can be rationalized in terms of an intrinsic nephelauxetic effect induced by the lone pairs of the lattice oxygens (Pauli repulsion), which strongly destabilize the K 4s level. This effect will depend of course upon the degree of interaction between the lone pairs and the K 4s orbital. A higher degree of interaction (i.e., an enhanced lone pair donaticity) will cause a greater destabilization of the K 4s orbital and as a consequence, reduced hyperfine splitting constants. This is indeed observed when K atoms are deposited on CaO and SrO. The differences in chemical reactivity and the well-known trend of basic strength of the alkaline earth oxides (MgO < CaO < SrO < BaO) have been

(55) Symons, M. C. R. *J. Chem. Soc.* **1964**, 1482.
(56) Murphy, D. M.; Giamello, E. *J. Phys. Chem.* **1994**, *98*, 7929.
(57) Murphy, D. M.; Giamello, E.; Zecchina, A. *J. Phys. Chem.* **1993**, *97*, 1739.
(58) Chiesa, M.; Paganini, M. C.; Giamello, E.; Murphy, D. M. *J. Phys. Chem. B*, **2001**, *105*, 10457.

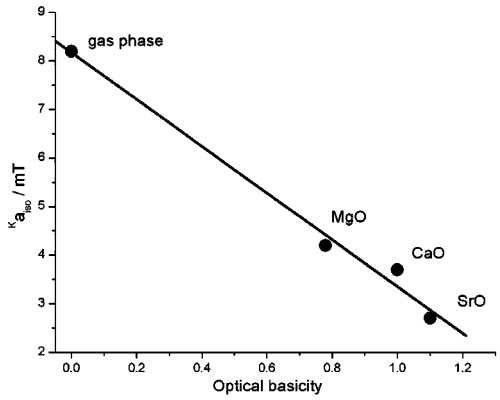

Figure 8. Optical basicity plotted against measured hyperfine coupling constants.

explained[16] considering the variation of the Madelung potential along the series. Lowering of the Madelung potential implies a reduced stabilization of the O^{2-} anion. This results in a more spatially diffuse charge distribution around the oxygen and to an enhanced propensity to donate electronic charge to adsorbed species.

A linear correlation is found between the ^{39}K hyperfine splitting on the different oxides and the so-called optical basicity (Λ) which can be taken as direct measure of the electron-donating power of oxygen in an oxide system,[59] Figure 8. Noteworthy, the extrapolation to "zero basicity" corresponds nicely to the gas phase K hyperfine constant, corroborating the self-consistency of the proposed analysis. This correlation has two important implications. First, it casts the role of K metal atoms as sensitive probes for the measure of the local Lewis basicity of insulating oxides. Second and most important, it demonstrates that the unpaired electron spin density, directly monitored via the EPR hyperfine splitting constant, is a very sensitive parameter to the degree of interaction between the metal and the oxide surface.

Borrowing again from the work on solvated alkali metal atoms,[45] a quantitative measure of this interaction can be obtained. As noticed by Catterall and Edwards[45] in the case of solvated alkali metals, the specific nature of the intrinsic nephelauxetic effect described above has the consequence of producing bound species with an electronic ground state which closely resembles that of an excited species in the gas phase. For both matrix-bound and excited S states of alkali metal atoms the electron density at the nucleus is a quantitative measure of the binding energy of the valence electron.

We may then use again the Kopfermann[54] equation as modified by Gupta[53] to relate the binding energy of the valence electron to the hyperfine coupling constant for excited S states of the alkalis. In this way, we can make a quantitative estimate, on a pure experimental basis, on how the surface to metal bonding interaction affects the ground state of the metal bound species. In particular, reduction of the electron spin density at the metal nucleus to 50%, 45%, and 32% of the gas phase value in the case of K atoms bound to MgO, CaO, and SrO respectively corresponds to a destabilization of the 4s orbital (SOMO) by ~1.8 eV, ~2.0 eV, and ~2.5 eV with respect to the gas-phase value. This implies that the IP of the surface bound metal species will be lowered more or less by the same amount

(59) Duffy, J. A.; Ingram, M. D. *J. Am. Chem. Soc.* **1971**, *93*, 6448.

which is in very good agreement with the calculations: the computed ΔIP is in fact 2.1 eV for MgO, 2.6 eV for CaO, and 2.8 eV for SrO, Table 5. We feel that the idea that the analogues of a gas-phase electronic excited species can be stabilized as a ground state on the surface of an oxide may prove to be important for the general understanding of the enhanced reactivity of metal atoms and clusters deposited on surfaces as well as alkali promotion and surface excitation effects.[60]

4. Conclusions

The interaction of K atoms with the surface of polycrystalline alkaline-earth metal oxides has been studied by means of combined CW and Pulse-EPR, UV−Vis−NIR spectroscopies and DFT cluster model calculations. Four main conclusions can be drawn. (1) K atoms are bound to oxide anions and stabilized at specific morphological sites by more than 1 eV, resulting in thermally stable species up to about 400 K. Despite its stability, the bonding between K and the oxide is neither a charge transfer interaction nor a classical covalent bond. Potassium atoms interact with oxide anions, with a bonding which has small covalent and large polarization contributions. The calculations show very clearly that the K atom is virtually neutral with the unpaired electron occupying its valence orbitals.,

(2) DFT analysis of different possible sites indicates that K atoms are bound at morphological defective sites. Among these sites, at least for MgO, anionc reverse corners, formed at the intersection of two steps are very likely candidates for the adsorption site.

(3) The interaction between K and the oxide surface results in a strong reduction of the $^{K}a_{iso}$ value, which goes from 8.2 mT for the free K atom to 2.7−4.1 mT on the oxide surfaces. Analysis of the EPR data and of the calculations shows that the strong reduction in a_{iso} is not connected to a delocalization of the spin density to other nuclei of the surface nor to a 4*s*−4*p* hybridization. Rather, it can be interpreted in terms of an intrinsic nephelauxetic effect, where the K 4s orbital becomes strongly destabilized by the interaction with the lattice oxygens. Similarly to classical solvation, the resulting species may be regarded to as an "expanded atom" and bears similarities to a gas-phase excited state. In this respect, we provide compelling evidence that a proper interpretation of the changes occurring in the $^{K}a_{iso}$ value going from a free atom to a molecular complex or to a surface species cannot be done by simple comparison of the respective isotropic coupling constants. It requires a careful analysis of all other magnetic interactions for correct evaluation of the spin density distribution, supported by quantum-mechanical calculations

(4) The hyperfine coupling constants of K atoms adsorbed on alkaline-earth oxides can be regarded to as an efficient "probe" to measure the degree of interaction between the metal and the surface. This latter is a direct function of the substrate basicity which increases going from MgO, to CaO and SrO. This view not only naturally explains the experimental facts, namely the modified spin distribution on the metal atom, the low hyperfine coupling constants on the surface oxygen ions and the red shift in the optical absorption band, but also reconciles the chemistry of the metal to surface interaction with the general problem of solvation providing a more general understanding of the chemical bond between metal atoms and oxide surfaces.

Acknowledgment. Financial support from the Italian Ministry of University and Research (Cofin 2003) is gratefully acknowledged.

Supporting Information Available: Hyperfine-decoupling experiments, HYSCORE simulation, temperature dependence of the CW-EPR spectra in the interval 4K−380K, computed properties of K atoms adsorbed at terraces of alkaline earth oxides. This material is available free of charge via the Internet at http://pubs.acs.org.

JA0542901

(60) Kotarba, A.; Adamski, G.; Sojka, Z., Witkowski, G.; Djega Mariadassou, G. *Stud. Surf. Sci. Catal*. **2000**, *130A*, 485.